



Analysis of abrasives on cutting edge preparation by drag finishing

Dejin Lv¹ · Yongguo Wang¹ · Xin Yu¹ · Han Chen¹ · Yuan Gao¹

Received: 29 June 2021 / Accepted: 21 December 2021 / Published online: 7 January 2022
© The Author(s), under exclusive licence to Springer-Verlag London Ltd., part of Springer Nature 2022

Abstract

Cutting edge preparation has become more important for tool performance. The micro-shape, radius and surface topography of the cutting edge play a significant role in the machining process. The cutting edge of solid carbide end mills has some micro-defects after grinding. For eliminating aforementioned problem, this study investigates drag finishing (DF) preparation for solid carbide end mills to reconstruct cutting edge micro-geometry. This paper is to present the design of DF experimental setup and analyze the characterization of various abrasive media (K3/600, K3/400, HSC 1/300 and HSO 1/100) on the evolution of the surface/roughness along the cutting edge. In parallel, the mechanism of material removal and the kinematics trajectory of the drag finishing are presented. In fact, the form factor (also called as “K-factor”) of the cutting edge micro-geometry is quantified. Comparing with four lapping media, the higher material removal rate (MRR) and the lower surface roughness are obtained by HSO 1/100 abrasive process. The results show that the cutting edge K-factor, MRR and surface topography are influenced by the abrasive particles size, composition and process time.

Keywords Drag finishing · Abrasive medium · K-factor · Kinematics trajectory · Cutting edge micro-geometry

1 Introduction

Solid carbide end mills mainly composed of carbide and cobalt, with high brittleness, have a complex helical surface, formation of micro-cracks, micro-chipping and sharp cutting edge after grinding [1–3]. In recent years, more and more scholars have paid attention to the impact of cutting edges on the tool. They found that sharp cutting edges were generally considered to be unfavorable for the cutting process because of their low stability and poor impact resistance [4, 5]. Denkena and Biermann [6] summarized cutting edge micro- and macro-geometry has a significant cutting performance. Thus, cutting edge preparation of solid carbide end mills has become an indispensable process, in order to reduce edge chipping at the beginning of the cutting process, increasing tool life and process reliability.

Drag finishing (DF) has a simple structure, has low cost, and can process multiple parts at the same time. It is also possible to polish workpieces with complex shapes, mainly used for deburring, cutting edge preparation and

high-demand polishing [7–9]. Uhlmann et al. [10] used DF equipment and various abrasives for preparing the micro-milling tools; the results obtained the cutting edge radius range from 4.0 μm to 31.2 μm . The crucial factors affecting the cutting edge preparation are the abrasive media. The removal of material mainly depends on the relative movement between the abrasive and the tool; the motion trajectory is epitrochoidal pattern [11]. During the DF process, Lin et al. [12] and Holzknecht [13] measured the final surface quality and material removal rate (MRR) by the abrasive dynamics and the initial surface roughness of the workpiece. The final surface is the result of three mechanisms: abrasive flow on the surface, media and workpiece interaction, abrasion chip formation, ploughing and cracking. The literature is very limited to characterize three types of mechanism.

Nguyen and Fang [14] studied silicon carbide (SiC) abrasive, which has stable chemical properties, high thermal conductivity, low thermal expansion coefficient, good wear resistance, and can be used as abrasive medium. Quartz, the main chemical component, is SiO_2 , which is an inorganic substance with very stable physical and chemical properties. Lee et al. [15] used silica (SiO_2) chemical mechanical polishing technology to establish a material removal rate distribution model. Nie et al. [16] summarized the shape and scale of complex abrasives, using digital image processing and B-spline

✉ Yongguo Wang
ygwang@shu.edu.cn

¹ School of Mechatronics Engineering and Automation, Shanghai University, Shanghai City 200072, PR China

generation techniques, which are accurately calculated particle shapes. Uhlmann et al. [17] used two different lapping medias (HSC1/300 (SiC) and H4/400 (walnut) experimental investigations on the preparation of four tool groups of micro-end mills' cutting edge geometry, the cutting edge radius r_β and the cutting edge chipping possibility to control the processing time t_B . Sooraj [18] dedicated the important issues of cutting edge preparation about abrasive media, due to the complex cutting tools and fixtures, cost-effectiveness, and surface finishing.

This article aims to provide a better understanding of mechanical removal mechanisms, with special emphasis on the role of abrasive media. The select of abrasive media is the key to the success of obtaining uniform cutting edge micro-geometry and topography. Hopefully, this paper will help provide some guidance on the tailored cutting edge preparations. According to experiments, most of the available research is deterministic and/or statistical, but there is less experience and less understanding of material removal and motion trajectory issues. Consequently, this paper presents a detailed drag finishing preparation process with four-kind abrasive medium in the mechanism of material removal and investigates the surface topography by SEM.

Nomenclature

| | | | |
|-----------|--|------------|-----------------------------|
| K | From factor | r_β | Cutting edge radius |
| $S\gamma$ | Cutting edge segment on the rake face | r_R | Sun wheel radius |
| $S\alpha$ | Cutting edge segment on the flank face | r_H | Planetary wheel radius |
| $A\gamma$ | Rake face | \bar{S} | Cutting edge rounding |
| $A\alpha$ | Flank face | β | Cutting edge wedge |
| φ | Apex angle | A_r | Material removal area |
| d_G | Abrasive grain diameter | θ | Rotation angle |
| n_R | Rotational speed of the first-planetary motion | r_s | Initial cutting edge radius |
| n_H | Rotational speed of the first-planetary motion | Δr | Profile flattening |

2 Materials and methods

2.1 Abrasives

In the process of cutting edge preparation, some scholars [19, 20] investigated the abrasive in the slurry, which plays a very important role in transferring mechanical energy to the machined surface. From the perspective of cutting edge preparation, abrasive media can be understood as the teeth of the tool in the cutting edge preparation. In this paper, the abrasive has no specific geometric and can be distinguished by the high hardness with sharp edges and also have good cutting abilities. Malkorra et al. [21] described the sharpness of abrasive particles including roundness and apex angle in detail. The abrasive

roundness model was according to the mathematical estimation method by [16, 21]. As the size of abrasive particles increased, the sharpness of the apex angles of these particles decreased, which reduced the cutting ability of the abrasives.

The abrasive of drag finishing with four different media, namely K3/600, K3/400 and HSC 1/300, was supplied by OTEC, Germany. The abrasive particles are observed by magnifying 100 as shown in Fig. 1. The abrasives of K 4/600 and K 4/400 are mainly composed of walnut shells, which are widely used because its high cost performance and relatively low wear and different sizes of walnut shells define different specifications. The above abrasives are all added with polishing paste containing diamond particles (in the range of a few microns), which are designed for rapid finishing and removal of large amounts of material. The HSC 1/300 abrasive in the experiments consists of 30% silicon carbide (SiC) and 70% walnut shell granulate of K3/400, which are widely used as cutting edge preparation. The novel abrasive of HSO 1/100 mainly consists of two components 50% SiO_2 and 50% walnut shell granulate of K3/400; its high hardness and material removal have unique performance in the cutting edge preparation process, which is also an important research in this paper. The physical properties of abrasive media are shown in Table 1. To compare the differences with abrasive during slurry, twenty end mills were prepared with each abrasive for five end mills.

2.2 Cutting tool

Solid carbide end mills are produced by ANCA TX7 + 5-axis CNC grinding machine. The 3D model of end mill is derived from the tool room grinding simulation software by ANCA as shown in Fig. 2a. After grinding, the marks and irregular

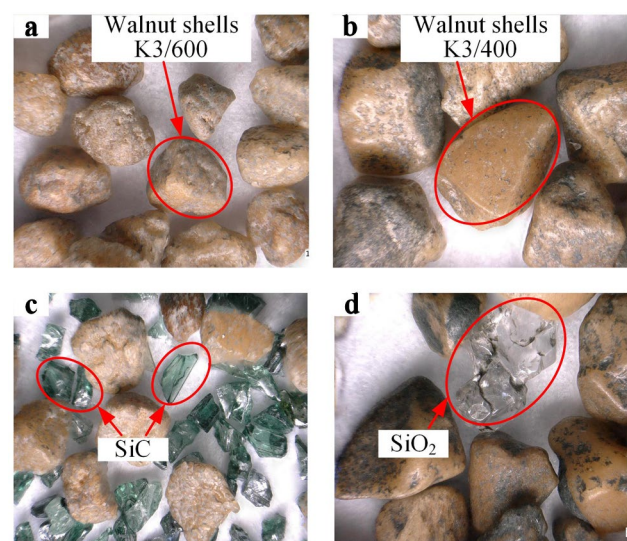


Fig. 1 Microscope images of abrasive particles

Table 1 Abrasive medium used for drag finishing

| Typical analysis | K 3/600 | K 3/400 | SiC | SiO ₂ |
|----------------------------------|-------------------------|-------------------------|--|---------------------------------|
| Hardness [(kg/mm ²)] | 1500 | 1500 | 2700 | 2400 |
| Density [g/cm ³] | 3.0 | 3.0 | 3.2 | 3.6 |
| Average diameter of grain [mm] | $0.4 \leq d_G \leq 0.8$ | $0.4 \leq d_G \leq 0.8$ | $0.4 \leq d_G \leq 0.8$ & $d_{SC} \approx 0.2$ | $0.8 \leq d_G, d_{SO} \leq 1.3$ |

defects are clearly visible. Irregular cutting edges in micro-geometry increase the stress concentration in the cutting process, leading to premature failure [1, 22, 23]. Weinert and Schneider [24] investigated that the grinding marks how to influence the chip flow, and the higher friction temperature and chip compression were observed. Lv et al. [3] reported that the size of W-Co grains correlated with a high degree of edge chipping, and the tool substrate of cobalt proportion results into the cutting edge roundness. In this paper, the uncoated solid carbide end mills with 8% Co content and average grain size of WC particles were measured to be about 0.6 μm as shown in Fig. 3. These end mills are in a four flute, six diameter with hardness HV = 1.7 kN/mm², supplied by Guohong Tool System (Wuxi) Co., Ltd. The milling tool geometric parameters are shown in Table 2.

The cutting edge micro-geometric characteristics are shown in Fig. 2b. As we all known, the edge radius r_β is normally characterized by the rounded cutting edges. But the micro-shape of cutting edge is actually not in a constant circle and cannot be characterized by only one parameter. Denkena and Biermann [6] established more precise characterization method with four parameters $S\gamma$, $S\alpha$, Δr , φ as presented in Fig. 2b. It is defined as the form factor method.

2.3 Drag finishing machine and parameters

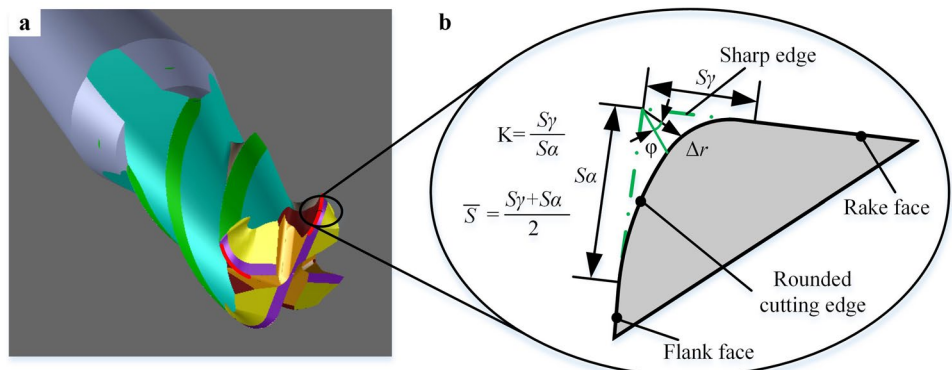
For the cutting edge preparation of solid carbide end mills with rounding cutting edge, drag finishing (DF) is an appropriate process. The DF machine is shown in Fig. 4a. DF-3 machine was made by the company OTEC PRÄZISIONS-FINISH GMBH, Straubenhardt, Germany. In the drag

finishing process, the milling tools were fixed on holders and immersed in the abrasive lapping medium. From Fig. 4a, the tools move along the two-stage planetary motion trajectory through the abrasive particles. The ability of material removal is the result of the relative movement between the cutter and the abrasive. The movement process is mainly driven by the spindle motor to drive the planetary motion to achieve both rotation n_R and revolution n_H movements.

The experimental analysis focuses on the cutting edge preparation by abrasive medium K3/600, K3/400, HSC 1/300 and HSO 1/100, which enhance MRR on the cutting edge; it can also achieve more efficient deburring and micro-defect. During the grinding process, surface quality, surface characteristics and surface texture of rake and flank faces play an essential role in solid carbide end mills performance. As Fig. 4c shows, the surface of the rake and flank face is obvious traces of the grinding wheel and micro-defects are obvious near the cutting edge. After preparation by HSO 1/100 abrasive, the micro-defect and grinding lines disappeared as shown in Fig. 4d.

All of the applied end mills have been produced out of one production batch with uncoated in Fig. 4b. The abrasives are listed in Fig. 1. The prepared cutting edges were labeled as E_i , where “i” depends on the abrasive medium indices for all prepared end mills. The unprepared solid carbide end mills E0 have an average cutting edge radius of $r_\epsilon = 3.35 \pm 0.58 \mu\text{m}$. For the investigations of four tool groups, each with five end mills was formed and each group has an abrasive preparation. The process parameters are given in Table 3. For all preparation parameters, the direction of rotor motion and the tools is clockwise for 1 min and counterclockwise for 1 min, and the total processing time is 20 min.

Fig. 2 (a) Solid carbide end mill and (b) K-factor of cutting edge characterization



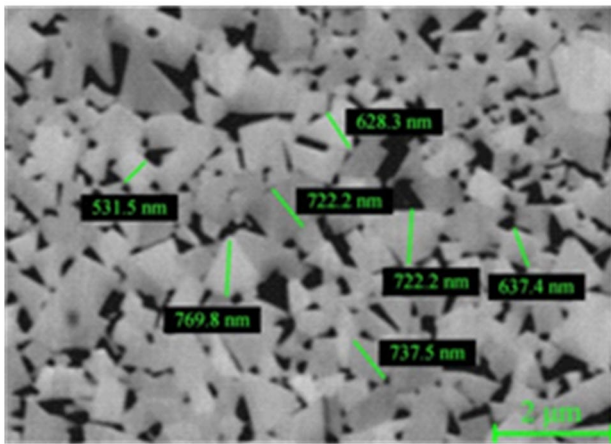


Fig. 3 The grain size of cemented carbide milling cutter

2.4 Cutting edge measurement

The edge geometry of all prepared solid carbide end mills is measured with Infinite-Focus G5 microscope by Alicona. The cutting edge micro-geometry was measured by built-in Edge Master Module and through the 50 edge profiles. As Fig. 5 shows, the green lines illustrate the fitting data. The four cutting edges of each tool are measured, and the average value is calculated and recorded. The entire cutting edge preparation process has a maximum deviation of 10% from the specified nominal rounding as mentioned by [25].

The surfaces' quality was done by quantitative analysis by Alicona G5. The cutting edge chipping measurement is automatically set along the cutting edge in the Edge Master Module. Moreover, some measurements with physical surface quality (arithmetic average height Ra , total height of profile peak and valley Rt and ten-point height Rz) have also obtained by Edge Master Module. The value Rt reflects the largest chipping of the cutting edge. The surface roughness qualitative analysis was used by scanning electron microscope (SEM) after drag finishing process of 20 min. Composed by five roughness profiles each, were performed on each sample, make sure the roughness profiles to be fixed in one positions.

Table 2 Solid carbide end mills geometric parameters

| Parameter | Value |
|------------------------------|-------|
| Shank diameter D | 8 mm |
| Tool diameter d | 6 mm |
| Number of teeth Z | 4 |
| Tool length L | 55 mm |
| Cutting edge length l | 10 mm |
| Helix angle β | 40° |
| Radial rake angle γ | 0° |
| Radial relief angle α | 8° |
| Corner radius R | 1 mm |

3 Results and discussion

3.1 Material removal process of DF

3.1.1 Analysis of abrasion mechanism

A basic understanding of material removal mechanisms is essential for developing predictive models and optimizing lapping processes. The function of solid particles in the slurry is to physically remove materials from the surface of the end mill. The material removal (MR) model of hard and brittle materials involved brittleness and ductility mechanisms, which depend on abrasive composition [26, 27]. During the movement of the abrasive and end mills, the contact between the particles and the cutting edges will only be established within a short period of time, resulting in impact and energy transfer, thereby smoothing the surface.

The impact removal mechanism of loose abrasive media on brittle materials in DF equipment can be divided into two types: brittle fracture and plastic deformation [28]. It involves two main crack systems, in which lateral cracks are responsible for material removal, while radial cracks lead to strength degradation in the red dotted line position as shown in Fig. 6. The latter is similar to the chip formation process in metal grinding, which involves scraping, ploughing and chip formation. Some assumptions based on the abrasive removal process are as follows:

- The abrasive particles are spherical and harder than the workpiece material.
- The movement of abrasive particles will not undergo plastic deformation or brittle fracture.
- No chemical reaction occurs on the particles and cutting edge contact interface.
- The crater produced by the crack propagation and chipping in brittle material is similar hemispherical shape.
- The processes of adhesion and deformation energy loss are independent.

According to this hypothesis, all materials, regardless of their hardness and brittleness, will undergo a transition from brittleness to ductile processing. Since the mode of deformation (plastic or brittle) depends on the state of stress and not on the magnitude of the stress, it is difficult to understand the local deformation caused by the material near the abrasion zone. The MR is based on the amount of the kinetic energy of the solid particle-impinged cutting edge equal to the energy of deformation. Therefore, the deformation energy of the MR can be determined by the incident energy of the solid particles and thus is defined as:

$$I_E = 0.5mv^2 \sin^2 \alpha (1 - e^2) \quad (1)$$

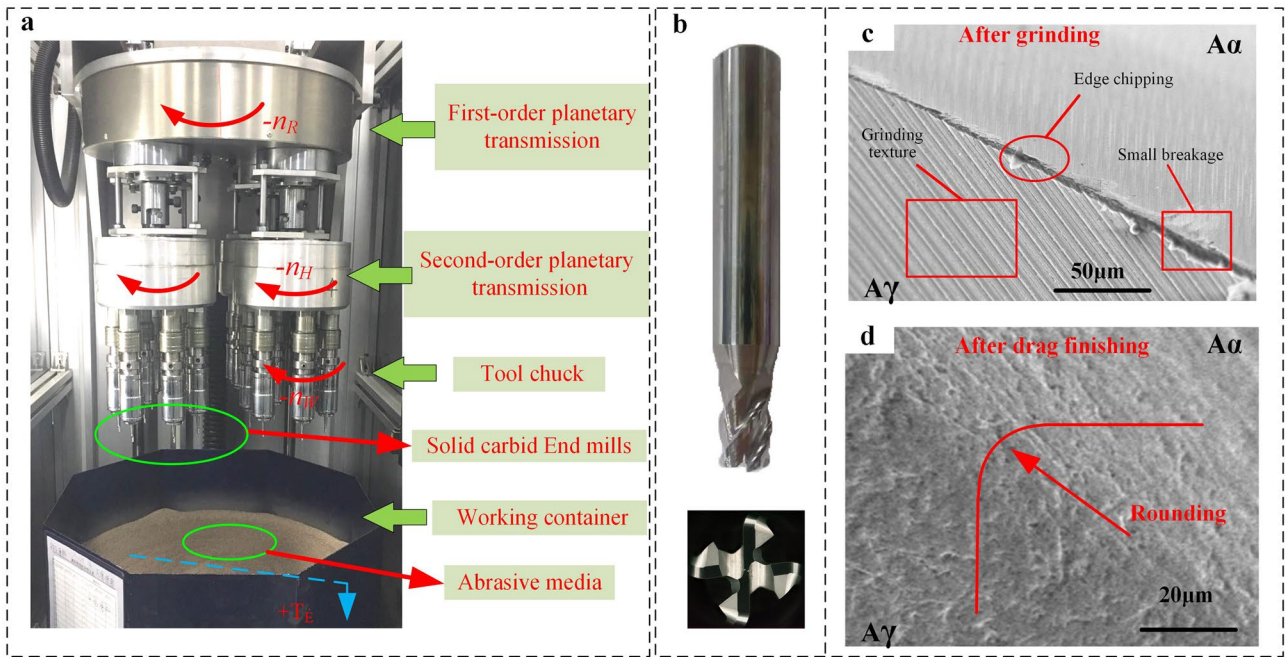


Fig. 4 DF process (a), DF machine (b), solid carbide end mills (c), cutting edge micro-defect after grinding (d) cutting edge rounding after HSO 1/100 abrasive preparation

where v and m are the impinging particle speed and mass, α the impact angle, and e the restitution coefficient, which can be estimated as follows:

$$e = \frac{1.7\sigma_{y-w}^{5/8}}{v^{1/4}\rho_a^{1/8}(E^*)^{1/2}} \quad (2)$$

where σ_{y-w} is the yield strength of the milling cutter, ρ_a the abrasive particle density, and E^* the equivalent modulus, that is:

$$\frac{1}{E^*} = \frac{1 - \nu_a^2}{E_a} + \frac{1 - \nu_w^2}{E_w} \quad (3)$$

where E_a and E_w are the elastic modulus of abrasive particle and milling cutter, and ν_a and ν_w are Poisson's ratios. Equation (3) provides an estimate of the material removal potential of solid particles during slurring.

Table 3 Process parameters for drag finishing

| Parameters | Vlue | Groupoup | Abrasive |
|--|------------|----------|----------|
| Rotational speed of the rotor n_R | 30 [r/min] | E1 | K 3/600 |
| Rotational speed of the workpiece hold n_H | 50 [r/min] | E2 | K 3/400 |
| Depth of immersion T_E | 20 [mm] | E3 | HSC1/300 |
| Processing time t_B | 20[min] | E4 | HSO1/100 |

When the particle movement has a high and positive strain hardening capability ($\delta\sigma/\delta\varepsilon > 0$, σ = flow stress, ε = plastic strain), the plastic deformation beneath the abrasives spreads uniformly for volume energy, as mentioned by [29, 30]. Conversely, if the kinetic energy of the particle does not exceed the tool material's strain or work hardening capacity ($\delta\sigma/\delta\varepsilon > 0$), the deformation under the particle is immediately confined to the near surface layer, leading to the formation of lip. Under this condition, the material deforms uniformly until the critical strain of $\delta\sigma/\delta\varepsilon = 0$. When high than this critical strain, $\delta\sigma/\delta\varepsilon < 0$, so the plastic deformation

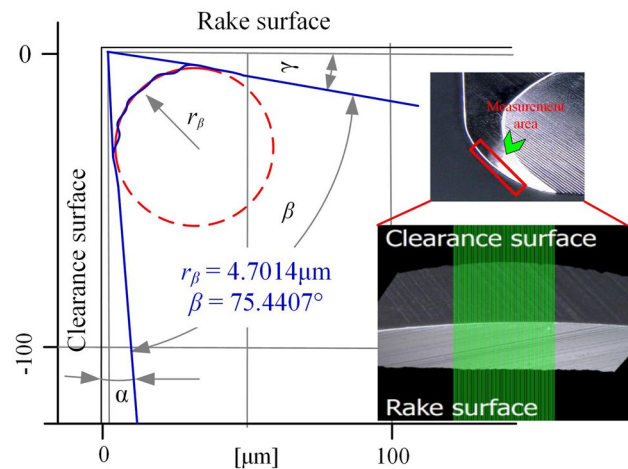


Fig. 5 Cutting edge measurement using Alicona microscope

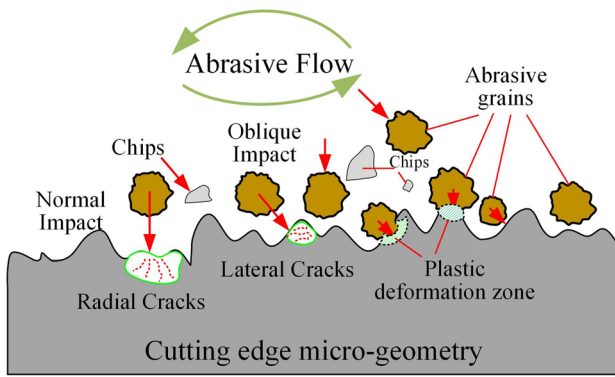


Fig. 6 Schematic illustration of the abrasive process

is localized to form a lip. As shown in previous studies [30], the plastic flow behavior of material deformation can be easily obtained, and the critical strain (ϵ_c) formed by the lip can be obtained. The following equations are related to flow stress (σ), plastic strain (ϵ) and temperature (T)

$$\sigma = K\epsilon^n(1 - CT) \tag{4}$$

where K is the strength coefficient, n is the strain hardening exponent and C is a constant characterizing the temperature dependence of the flow stress. The critical strain for localization and hence lip formation (ϵ_c) is then obtained as

$$\epsilon_c = \left(\frac{n\rho_w C_{p-w} (T_m/K)}{CT_m} \right)^{1/(n+1)} \tag{5}$$

where n is strain hardening exponent, ρ_w is cutter material density, C_{p-w} and T_m are the specific heat and melting point, respectively, of the abrasive and C is constant which has about 0.5 for many typical metals, as reported by [31].

3.1.2 Drag finishing kinematics analysis

The two-stage planetary motion of the tool is shown in Fig. 7a. In Fig. 7a, ω_1 is the rotation speed of axis O_2 around

Fig. 7 Drag finishing motion analysis: (a) motion diagram and (b) milling cutter movement trajectory

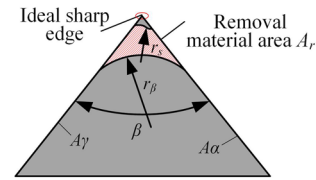
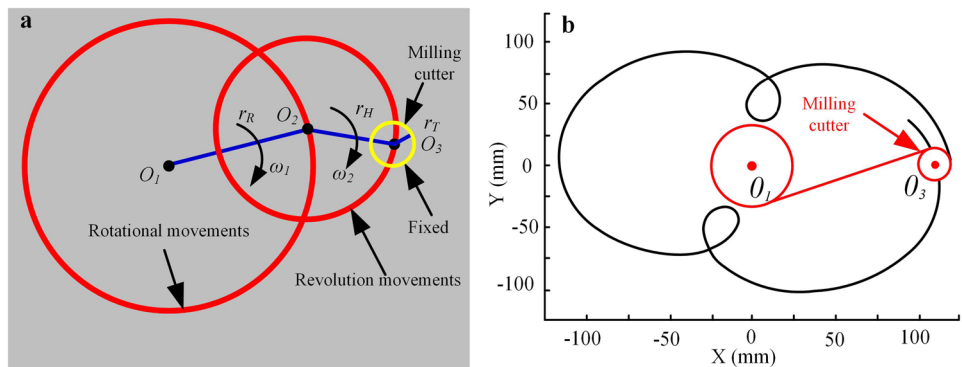


Fig. 8 Concept of nominal removed area A_r

O_1, ω_2 is the rotation speed of axis O_3 around O_2 , r_R is the rotation radius of O_2 , r_H is the rotation radius of O_3 , and r_T is the tool rotation radius. The pattern of a generic point on the outer surface of the milling cutter during its motion can be accurately described by the following Eq. (6):

$$\begin{cases} x(\theta) = (r_R + (r_H + i)) \cos \theta - d \cdot \cos\left(\frac{r_R + (r_H + i)}{(r_H + i)} \theta\right) \\ y(\theta) = (r_R + (r_H + i)) \sin \theta - d \cdot \sin\left(\frac{r_R + (r_H + i)}{(r_H + i)} \theta\right) \end{cases} \tag{6}$$

With this particular motion, the tools' movement trajectory by MATLAB 7.0 is shown in Fig. 7b. An epicycloid trajectory ensures the maximum contact uniformity between the abrasive and the tool surface, accordingly, which is the best performance of the drag finishing.

3.1.3 Material removal rate (MRR)

In order to characterize the precision removal process for cutting edge preparation, a parameter can be defined as A_r nominal removal area in Fig. 8. Regardless of the length of the cutting edge, the number of five tools is processed simultaneously. The A_r determines the material removal in the preparation of the cutting edge and represents the nominal initial radius r_s for transforming final radius r_β to remove the area of material. The four abrasive removal capabilities are shown in Fig. 9.

The nominal removed area A_r can be written as follows:

$$A_r = K_\beta (r_\beta^2 - r_s^2) \tag{7}$$

where K_β is:

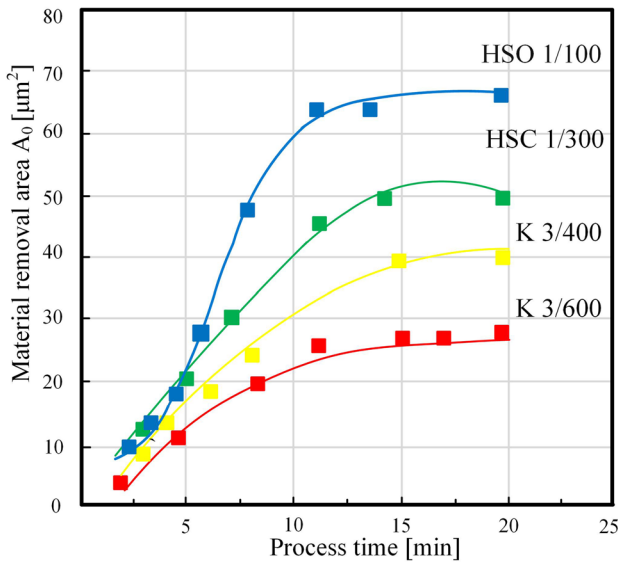


Fig. 9 Material removal area of four abrasives with the time variation

$$K_\beta = \frac{\sin^2\left(90^\circ - \frac{\beta}{2}\right)}{\tan\frac{\beta}{2}} - \frac{\pi}{2} \left(\frac{180^\circ - \beta}{180^\circ}\right) + \sin(180^\circ - \beta) \tag{8}$$

K_β is the coefficient of function of the wedge angle β .

3.2 Cutting edge characterization

3.2.1 Cutting edge K-factor parameters

The macroscopic and microscopic geometry defines the shape of cutting tool. The micro-geometry characterizes the cutting edge, which is the transition between the rake face and flank face to the cutting wedge. For the rounded cutting edge, the radius (r_β) is still frequently used to characterize the cutting edge micro-geometry. Generally, the fitting shape of the cutting edge is not circular, and it is too simple to use a single parameter to characterize it. Denkena and Biermann [6] established the form-factor method (also referred to as K-factor method), which more accurately describes the cutting edge micro-geometry; it can be measured by the Alicona Infinite Focus microscope.

The K-factor of cutting edges is prepared by four-level abrasive medium on the process time. For each section of lapping media, the average cutting edge rounding \bar{S} is calculated from Edge Master Module to fitting 50 edge contours. At the same time, the length of cutting edge $S\alpha$ and $S\gamma$ is introduced to measure the distance between the ideal sharp cutting edge and flank face and rake face, respectively. The location of the tangent separation of $S\alpha$ and $S\gamma$ largely depends on the fitting area. The K-factor reflects the cutting

edge with symmetry and asymmetry. As for asymmetry cutting edge ($K < 1$) defined as waterfall hone and ($K > 1$) defined as trumpet hone and as for symmetry cutting edge defined as ($K = 1$), Fig. 10 demonstrates the K-factor parameters with four abrasives at process time of 20 min. It can be seen from the figure that the HSO 1/100 abrasive has the highest removal ability after processing time of 20 min, and it can be considered for large K-factor value. The scope of application of this abrasive will be description in my article. At process parameters, $n_H = 30$ rpm, $n_R = 100$ rpm and $T_E = 30$ mm, the K-factor variation ranges from 0.9 to 1.2, because the symmetrical cutting edge is a commonly prepared parameter in the case of proportional clockwise and counterclockwise rotations. The cutting edge rounding \bar{S} values approximately range from 5 μm to 10 μm after process time of 20 min. The stability of MR mainly comes from the consistency abrasive, while tolerances on the cutting edge geometry and the positioning are somewhat relaxed. The micro-geometry and surface finish depend on the size and component of the abrasive particle.

3.2.2 Cutting edge radius

According to the research in the previous section, the symmetrical cutting edge is the main goal of this paper. Although the cutting edge radius r_β is too simplified, it is still very common in practical applications. The accuracy of cutting edge depiction with a constant circle can be increased by using a higher number of measured points.

The characterization accuracy of the cutting edge radius depends on the selection of the measuring point, which determines the fitting constant circle. Benjamin and Thilo [32] and Wyen [33] indicated that fitting algorithm was also

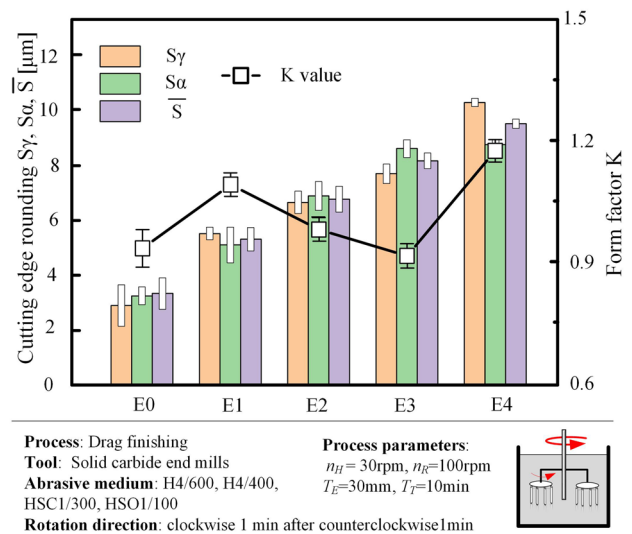
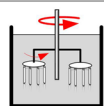


Fig. 10 K-factor by drag finishing for solid carbide end mills



a very important factor. The unprepared cutting edges (r_s) is in the range of $3 \mu\text{m} < r_s < 5 \mu\text{m}$. The abrasive removal process is shown in Fig. 6. By calculating the mean value and standard deviation of all prepared cutting edge radius, it is possible to evaluate the repeatability of abrasive process. The unprepared cutting edges have some micro-defects and grinding marks clearly visible on the rake and flank surfaces. All these edge defects can cause large deviations in the measurement along the cutting edge and lead to reduced cutting stability and tool life. It can be seen from Fig. 11 that the cutting edges prepared by four abrasives have prepared different cutting edge radii. Among them, the K3/600 abrasive preparation r_β is the smallest, so that the normal distribution is dispersed, while the novel HSO1/100 abrasive obtains the largest r_β , and the passivation value is less fluctuate, which indicates that the prepared cutting edge is more uniform. The cutting edge radii prepared by HSC1/300 and HSO1/100 abrasives are uniformly distributed, and the mean values are 12 and 15 μm , respectively. Because SiO_2 has a higher hardness, adding 50% fine grain SiO_2 to K3/400 walnut powder has a higher abrasion ability to obtain a larger edge radius. Regarding the application of four abrasives, the abrasives should be tailored specific processing materials and working conditions.

3.3 Surface topography

3.3.1 Abrasive process

As we all know, the preparation of the cutting edge is not only a process of changing the cutting edge geometry, but also a process that modifies the surface topography. Figure 12a depicts a schematic diagram of microscopic damage such as burrs and chipping. Commonly used abrasives are HSC 1/300, H4/400 and M4/400, which are one of the most popular abrasive used for the preparation of the cutting edge [17]. The surface roughness variation caused by the interaction of solid particles and the cutting edge surface are quantitative analysis by the parameters Ra , Rz and Rt . In the DF finishing

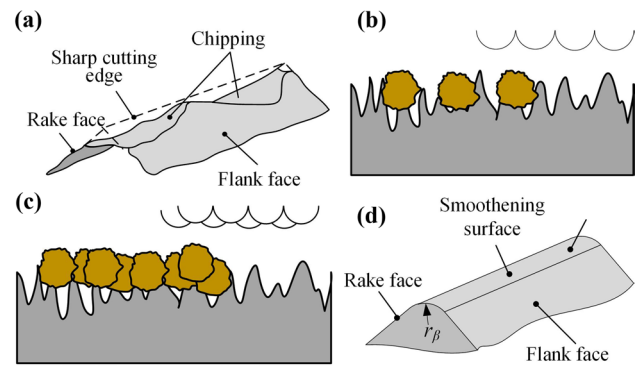


Fig. 12 Schematic diagram of surface smoothing process: (a) cutting edge micro-defect after grinding, (b) single abrasive impact, (c) multiple, repeated impacts of abrasive impact, (d) smooth surface after certain process time

process, the abrasion caused by plastic deformation/indentation or micro-cracks in the case of brittle materials is regarded as a hemispherical volume, as shown in Fig. 12b. As shown in Fig. 12c, multiple abrasive particles overlap the cutting edge, resulting in a smooth surface and rounded cutting edge as seen in Fig. 12d.

3.3.2 Cutting edge surface roughness

This section mainly analyzes the cutting edge surface roughness prepared by the four kinds of abrasives. Denkena and Biermann [6] showed that the surface roughness of the cutting edge is very important for the chip flow, cutting force and temperature distribution in the cutting area, especially for coated cutting tools. Therefore, evaluation of the cutting edge surface quality after four kinds of abrasive mediums that prepared cutting edge roundness is of great significance. In this way, successive cross sections of the cutting edge roughness can be monitored; variation of average roughness Ra , Rz and Rt , after drag finishing, can be estimated. Out of the large number of experiments conducted, 2D profile of cutting edge is selected for relatively stable cutting edge of solid carbide end mill, as presented in Fig. 13. The measurement of the edge chipping is summarized in Fig. 14. As the size of the larger rounding increases, the chipping Rt decreases. The error bars in the figure represent the standard deviation of the measurements. In order to prove the repeatability of the microscopic geometry, the cutting edge prepared by each abrasive was measured three times.

Notably, the roughness Ra and Rz decrease with different abrasives. Since the removal of material depends on the interaction between the tool and the solid particles of the abrasive, the height and distance between the peaks are significantly decreased. This is because the solid abrasive is squeezed to remove micro-defects on the cutting edge surface and removes surface peaks in each process. As explained

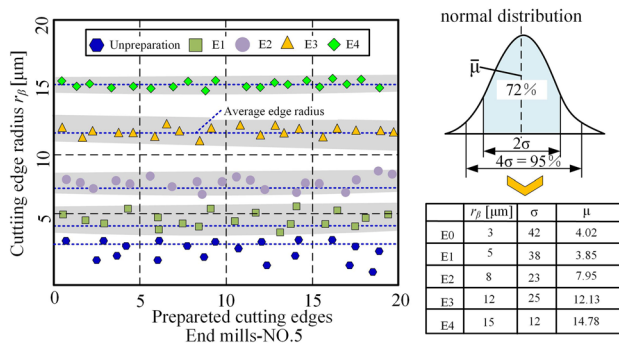
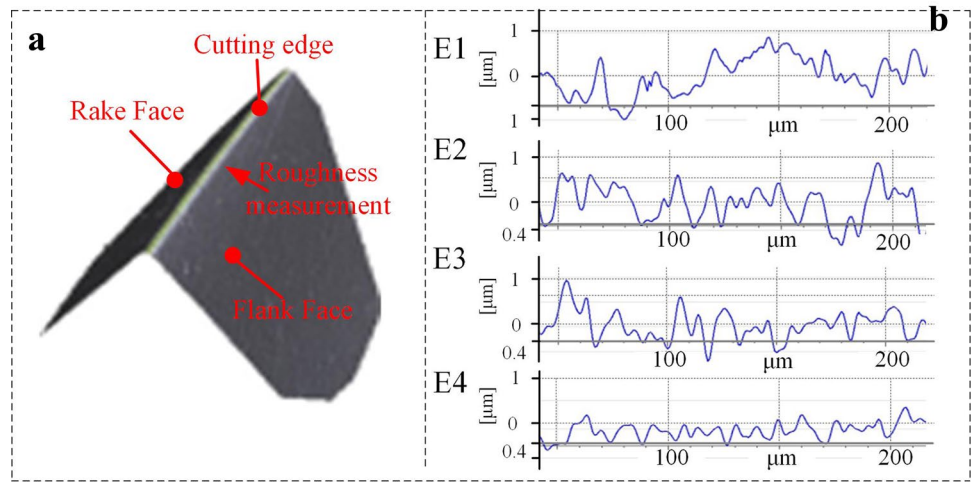


Fig. 11 Cutting edge radius after abrasive process

Fig. 13 The cutting edge roughness measurement: (a) cutting edge 3D topography; (b) cutting edge 2-D profile



by the previous theory, De Pellegrin and Stachowiak [28] clearly proved the effectiveness of elastic abrasion. The critical values of R_t after a processing time of 20 min are E0: $3.5 \pm 0.1 \mu\text{m}$, E1: $1.8 \pm 0.85 \mu\text{m}$, E2: $1.36 \pm 0.53 \mu\text{m}$, E3: $2.0 \pm 0.53 \mu\text{m}$ and E4: $0.9 \pm 0.53 \mu\text{m}$, respectively. This is because the removal ability of different abrasive media, including abrasive geometry, composition and kinetic energy vibration and fluctuations in the abrasion process.

In Fig. 15, the surface roughness quantitative analysis of the cutting edge prepared by K3/600, K3/400, HSC 1/300 and HSO 1/100 abrasives is measured. Experimental results show that the abrasive HSO 1/100 mixed SiO_2 abrasive 50% exhibits a smaller average surface roughness (R_a). Beucamp et al. [26] recognized the solid carbide tools in the form of brittleness removal during the cutting edge preparation process, and the surface was smoothed on and around the cutting edge. The surface roughness value of all prepared cutting edges is lower than the unprepared edge. It can be observed that cutting

edge roughness decreased by HSO 1/100 abrasive medium preparation. It is due to the larger material removal ability; the micro-defect disappeared with increasing cutting edge radius and obtained the better surface quality.

3.3.3 Cutting edge micro-topography

In order to do further qualitative analysis of the influence of drag finishing on the surface structure of solid carbide end mills, SEM was used to measure the cutting edge morphology using EVO 18 Zeiss. Solid carbide end mills are prepared by four abrasives in Table 3. As mentioned by Bouzakis et al. [34] and other relative works by Ricardo and Sommerfeld [35], sharp cutting edge of solid carbide end mills without drag finishing treatment has irregular shapes and micro-defect as shown in Fig. 12a. Cutting edge micro-topography describes the surface structure of the cutting edge, as shown in Fig. 16. In the corresponding SEM-supported investigations, the rake face and flank face near the cutting edge were smooth after HSO 1/100 abrasive prepared E4 group end mills; no

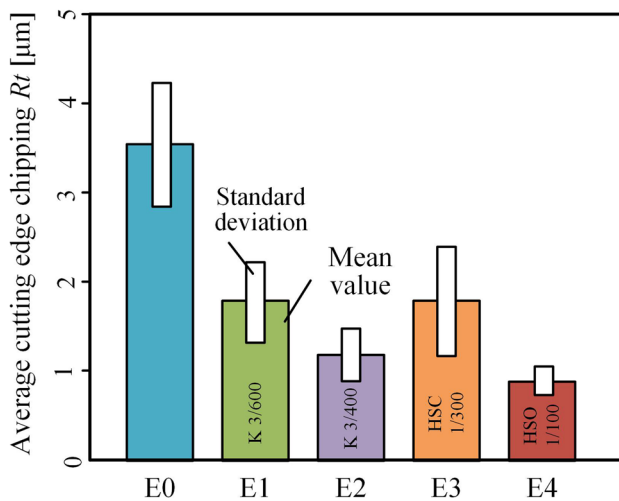


Fig. 14 Average cutting edge chipping R_t after drag finishing

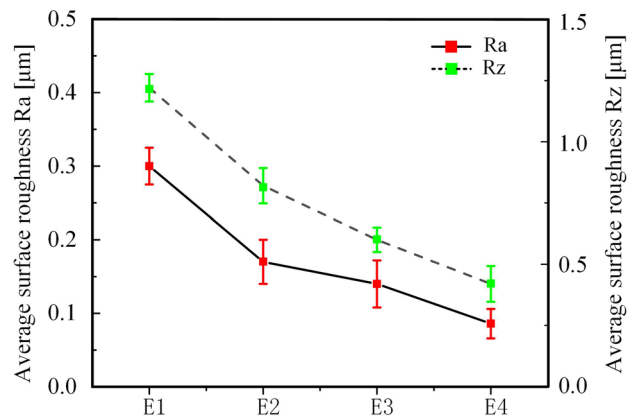


Fig. 15 Cutting edge roughness R_a and R_z

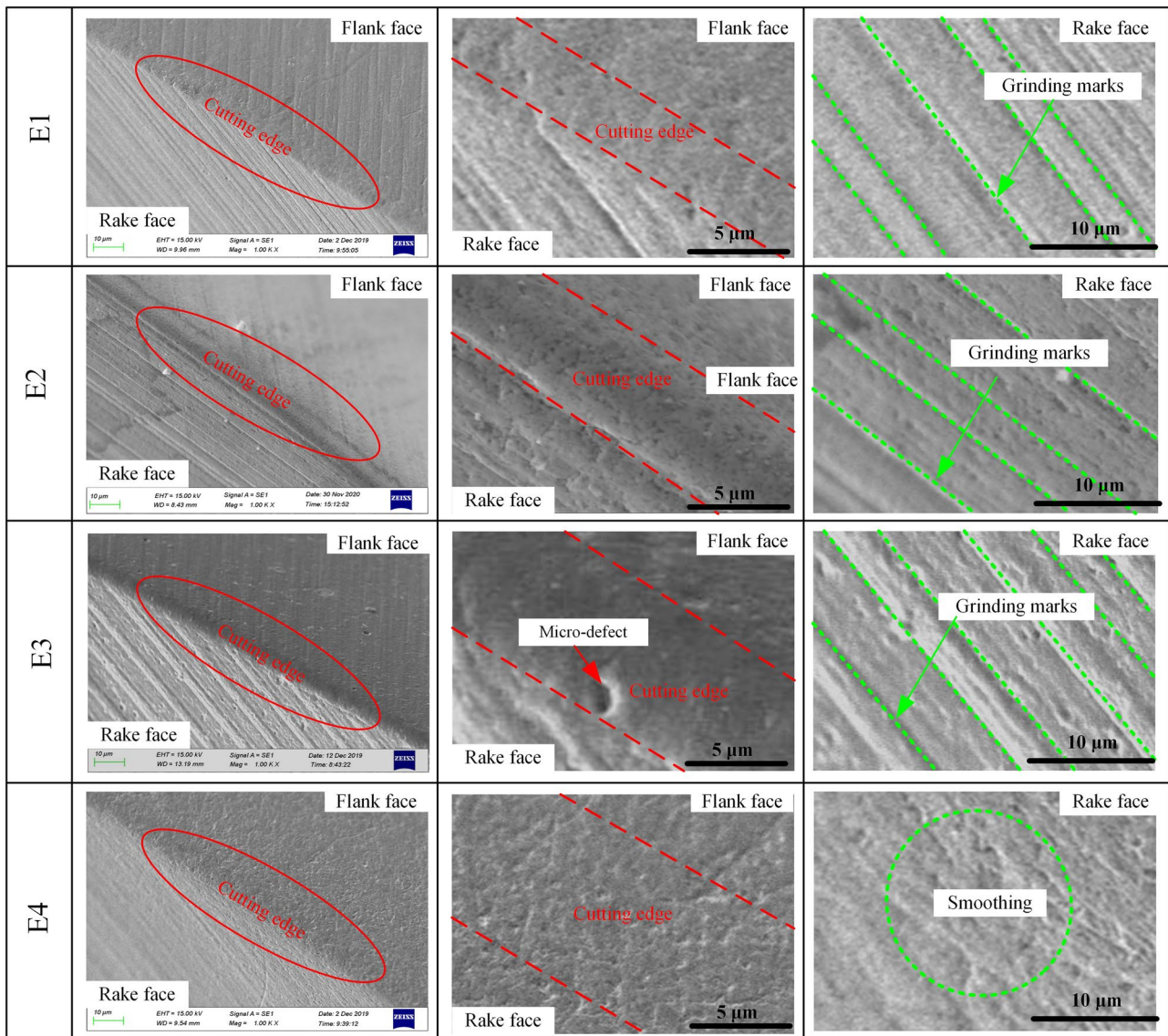


Fig. 16 SEM micro-graphs of four prepared solid carbide end mills

obvious signs of micro-breakages and consistent cutting edge micro-geometry were obtained. By observing other abrasives to prepare the cutting edge, the micro-morphology of the cutting edge has not been well improved. Comparing K3/600, K3/400 and HSC1/300 abrasives to prepare solid carbide end mills E1, E2 and E3, the cutting edges micro-geometry and topography structure are all processed, but the grinding track is still clearly visible on the rake face. As we all know, the roughness of the rake face was greatly significant and the chip flow and the quality of cutting edge thus affect the tool life. This paper researches the process of abrasive to prepare the cutting edges, but for coated tools, it is necessary to combine the tool coating for tailoring the preparation technics to

enforce its performance. In the future, the interaction between the cutting edge and the combination of tool wear and life will respect to the attention of the scientists.

4 Conclusions

This paper uses different abrasive media to prepare solid carbide end mills by drag finishing on the mechanism of movement trajectory, material removal, cutting edge characterization, and surface topography. The results showed the comprehensive abrasive machining process and characterization method of cutting edge by K-factor parameters ($S\alpha$, $S\gamma$, $K\bar{S}$).

- The mechanism of material removal and trajectory motion by drag finishing with two-stage planetary motion was obtained. Material removal volume A_r uses four abrasives (K3/600, K3/400, HSC 1/300 and HSO 1/100) to analyze the ability of removal material after process time of 20 min.
- The geometric characterization measured by Edge Master Module after abrasive machining process revealed different shapes and sizes (average cutting edge rounding \bar{S} ranges from 5 to 10 μm).
- With the proper selection of the abrasives process of cutting edge preparation, the abrasive HSO 1/100 is possible to achieve the highest cutting edge radius r_β with 15 μm and the required high quality of their surface.
- The quantitative description of cutting edge surface topography (R_a , R_z and R_t) by four abrasive preparations. Compared to four abrasives HSO 1/100 has obtained better smoothness. The application of abrasives is very important in the preparation of cutting edges in solid carbide end mills. Therefore, the study of analysis of the abrasives in cutting edge preparation should be extended, taking into account the variability of various machining parameters, which is the purpose of further research.

Acknowledgements The authors would like to thank the Guohong tool system (Wuxi) Co., Ltd. for providing the experimental conditions, including drag finishing and cutting experimental devices, tools, workpiece materials, etc.

Author contribution The first author Lv DJ has been responsible for writing this paper, testing and collecting experimental data, analysis varies abrasives on preparation of cutting edge, researching the removal mechanism of abrasives. Yu X is responsible for conducting a theoretical model research in the abrasive process. Chen H is responsible for verification, whether as a part of the activity or separate, of the overall reproducibility of results and the cutting edge measurement. Gao Y is responsible for formulation or evolution of overarching research goals and aims. The corresponding author Wang YG is responsible for determining the overall logical structure of the paper and guiding the entire experiment.

Declarations

Ethics approval Ethics approval was not required for this research.

Consent to participate Not applicable.

Consent for publication The authors do agree that the copyright of this paper is transferred to Springer's journal "The International Journal of Advanced Manufacturing Technology" when the paper is accepted for publication.

Competing interests The authors declare that they have no conflict of interest.

References

1. Denkena B, Michaelis A, Herrmann M, Pötschke J, Krödel A, Vornberger A, Picker T (2020) Influence of tool material properties on the wear behavior of cemented carbide tools with rounded cutting edges. *Wear* 15:456–457. <https://doi.org/10.1016/j.wear.2020.203395>
2. Li GC, Sun J, Li JF (2014) Modeling and analysis of helical groove grinding in end mill machining. *J Mater Process Technol* 214:3067–3076. <https://doi.org/10.1016/j.jmatprotec.2014.07.009>
3. Lv DJ, Wang YG, Yu X (2020) Effects of cutting edge radius on cutting force tool wear and life in milling of SUS-316L steel. *Int J Adv Manuf Technol* 111:2833–2844. <https://doi.org/10.1007/s00170-020-06286-7>
4. Bergmann B, Denkena B, Grove T, Picker T (2019) Chip formation of rounded cutting edges. *Int J Precis Eng Manuf* 20(2). <https://doi.org/10.1007/s12541-019-00020-4>
5. Padmakumar M, Shiva PN (2020) Effect of cutting edge form factor (K-factor) on the performance of a face milling tool. *CIRP J Manuf Sci Technol* 31(4). <https://doi.org/10.1016/j.cirpj.2020.06.004>
6. Denkena B, Biermann D (2014) Cutting edge geometries. *CIRP Ann* 63:631–653. <https://doi.org/10.1016/j.cirp.2014.05.009>
7. Barletta M, Rubino G, Valentini PP (2015) Experimental investigation and modeling of fluidized bed assisted drag finishing according to the theory of localization of plastic deformation and energy absorption. *Int J Adv Manuf Technol* 77:2165–2180. <https://doi.org/10.1007/s00170-014-6620-y>
8. Qi H, Qin SK, Cheng ZC, Zou YL, Cai DH, Wen DH (2021) DEM and experimental study on the ultrasonic vibration-assisted abrasive finishing of WC-8Co cemented carbide cutting edge. *Powder Technol* 378:716–723. <https://doi.org/10.1016/j.powtec.2020.10.043>
9. Zhuang KJ, Fu CN, Weng J, Hu C (2021) Cutting edge microgeometries in metal cutting: a review. *Int J Adv Manuf Technol* 116:2045–2092. <https://doi.org/10.1007/s00170-021-07558-6>
10. Uhlmann E, Oberschmidt D, Löwenstein A, Kuche Y (2016) Influence of cutting edge preparation on the performance of micro milling tools. *Procedia CIRP* 46:214–217. <https://doi.org/10.1016/j.procir.2016.03.204>
11. Barletta M, Gisario A, Venettacci S, Rubino G (2014) A comparative evaluation of fluidized bed assisted drag finishing and centrifugal disk dry finishing. *Eng Sci Technol Int J* 17(2):63–72. <https://doi.org/10.1016/j.jestech.2014.03.007>
12. Lin B, Jiang XM, Cao ZC, Huang T, Li KL (2019) Theoretical and experimental analysis of material removal and surface generation in novel fixed abrasive lapping of optical surface. *J Mater Process Technol* 279:116570. <https://doi.org/10.1016/j.jmatprotec.2019.116570>
13. Holzknacht E (2014) Drag finishing displaces manual and robotic grinding & polishing. *MFN Metal Finishing News*
14. Nguyen VT, Fang TH (2020) Material removal and wear mechanism in abrasive polishing of SiO₂/SiC using molecular dynamics. *Ceram Int* 46:21578–21595. <https://doi.org/10.1016/j.ceramint.2020.05.263>
15. Lee HS, Jeong HD, Dornfeld DA (2013) Semi-empirical material removal rate distribution model for SiO₂ chemical mechanical polishing (CMP) processes. *Int J Precis Eng* 37:483–490. <https://doi.org/10.1016/j.precisioneng.2012.12.006>
16. Nie ZH, Liang ZY, Wang X, Gong J (2018) Evaluation of granular particle roundness using digital image processing and computational geometry. *Constr Build Mater* 172:319–329. <https://doi.org/10.1016/j.conbuildmat.2018.03.246>

17. Uhlmann E, Oberschmidt D, Kuche Y, Löwensteinb A (2014) Cutting edge preparation of micro milling tools. *Procedia CIRP* 14:349–354. <https://doi.org/10.1016/j.procir.2014.03083>
18. Sooraj VS (2017) On the process and mechanics of rotary elasto-abrasive finishing. *Mach Sci Technol* 21 474–492. <https://doi.org/10.1080/10910344.2017.1284565>
19. Salvatore F, Grange F, Kaminski R, Claudin C, Kermouche G, Rech J, Texier A (2017) Experimental and numerical study of media action during tribofinishing in the case of SLM titanium parts. *Procedia CIRP* 58:451–456. <https://doi.org/10.1016/j.procir.2017.03.251>
20. Evans CJ, Paul E, Dornfeld D, Lucca DA, Mullany BA (2003) Material removal mechanisms in lapping and polishing. *CIRP Ann* 52:611–633. [https://doi.org/10.1016/S0007-8506\(07\)60207-8](https://doi.org/10.1016/S0007-8506(07)60207-8)
21. Malkorra I, Salvatore F, Rech J, Arrazola P, Tardelli J, Mathis A (2020) Influence of lubrication condition on the surface integrity induced during drag finishing. *Procedia CIRP* 87:245–250. <https://doi.org/10.1016/j.procir.2020.02.087>
22. Toenshoff HK, Denkena B (2013) Basics of cutting and abrasive processes. Springer Verlag. <https://doi.org/10.1007/978-3-642-33257-9>
23. Barbosa M, Hassui A, Oliveira PAD (2021) Effect of cutting parameters and cutting edge preparation on milling of VP20TS steel. *Int J Adv Manuf Technol* 116(9–10). <https://doi.org/10.1007/s00170-021-07654-7>
24. Weinert K, Schneider M (2000) Simulation of tool-grinding with finite element method. *CIRP Ann* 49:253–256. [https://doi.org/10.1016/S0007-8506\(07\)62940-0](https://doi.org/10.1016/S0007-8506(07)62940-0)
25. Zhao T, Zhou JM, Bushlya V, Ståhl JE (2017) Effect of cutting edge radius on surface roughness and tool wear in hard turning of AISI 52100 steel. *Int J Adv Manuf Technol* 88(9–12):1–8. <https://doi.org/10.1007/s00170-017-0065-z>
26. Beaucamp A, Simon P, Charlton P, King C, Matsubara A, Wegener K (2016) Brittle-ductile transition in shape adaptive grinding (SAG) of SiC aspheric optics. *Int J Mach Tools Manuf*. <https://doi.org/10.1016/j.ijmactools.2016.11.006>
27. Lin B, Jiang XM, Cao ZC, Huang T, Li KL (2019) Theoretical and experimental analysis of material removal and surface generation in novel fixed abrasive lapping of optical surface. *Mater Process Technol* 279:1165–1170. <https://doi.org/10.1016/j.jmatprotec.2019.116570>
28. De Pellegrin DV, Stachowiak GW (2002) Assessing the role of particle shape and scale in abrasion using sharpness analysis: Part I. Technique development. *Wear* 253(9–10):1016–1025. [https://doi.org/10.1016/S0043-1648\(02\)00232-6](https://doi.org/10.1016/S0043-1648(02)00232-6)
29. Brach RM (1988) Impact dynamics with applications to solid particle erosion. *Int J Impact Eng* 7:37–53. [https://doi.org/10.1016/0734-743X\(88\)90011-5](https://doi.org/10.1016/0734-743X(88)90011-5)
30. Sundararajan G (1991) A comprehensive model for the solid particle erosion of ductile materials. *Wear* 149:111–127. [https://doi.org/10.1016/0043-1648\(91\)90368-5](https://doi.org/10.1016/0043-1648(91)90368-5)
31. Fowler G, Pashby IR, Shipway PH (2009) The effect of particle hardness and shape when abrasive water jet milling titanium alloy Ti6Al4V. *Wear* 266:613–620. <https://doi.org/10.1016/j.wear.2008.06.013>
32. Benjamin B, Thilo G (2018) Basic principles for the design of cutting edge roundings. *CIRP Ann* 67:73–78. <https://doi.org/10.1016/j.cirp.2018.04.019>
33. Wyen CF (2011) Rounded cutting edges and their influence in machining titanium. (PhD-Thesis) ETH Zürich
34. Bouzakis KD, Michailidis N, Skordaris G, Bouzakis E, Biermann D, M'Saoubi R (2012) Cutting with coated tools: coating technologies characterization methods and performance optimization. *CIRP Ann* 61:703–723. <https://doi.org/10.1016/j.cirp.2012.05.006>
35. Ricardo GAN, Sommerfeld M (2020) Experimental evaluation of surface roughness variation of ductile materials due to solid particle erosion. *Adv Powder Technol* 31:3790–3816. <https://doi.org/10.1016/j.apt.2020.07.023>

Publisher's Note Springer Nature remains neutral with regard to jurisdictional claims in published maps and institutional affiliations.